

Constraints on cosmic-ray interaction and propagation within the HB3/W3 complex using *Fermi*-LAT data

Aimie Clément,^{a,b,*} Marianne Lemoine-Goumard,^a Valentine Wakelam,^b Patrick Slane^c and Pierre Gratier^b on behalf of the *Fermi*-LAT collaboration

^aUniversité de Bordeaux, CNRS, LP2I Bordeaux, UMR 5797, F-33170 Gradignan, France

^bLaboratoire d'Astrophysique de Bordeaux (LAB), Univ. Bordeaux, CNRS, B18N, allée Geoffroy Saint-Hilaire, 33615 Pessac, France

^cCenter for Astrophysics, Harvard Smithsonian, 60 Garden St, Cambridge, MA 02138, USA

E-mail: aimie.clement@u-bordeaux.fr, lemoine@cenbg.in2p3.fr

Diffusive shock acceleration in supernovae can accelerate particles to very-high energies (VHE, $E > 100$ GeV). HB3 is a supernova remnant (SNR) detected by the *Fermi* Large Area Telescope in 2016 with 6 years of data, adjacent to the south-eastern part of the giant HII complex W3. The low energy γ -ray emission of both systems shows a clear signature of proton acceleration. Here we use a significantly larger dataset of 14 years of data with the improved P8R3 instrument response functions to perform a precise morphological study of the SNR and W3 above 1 GeV using multi-wavelength data in the X-ray and radio bands. This allows us to derive the spectra of both systems above 100 MeV. In this presentation, we will review the consequences of this precise analysis providing new constraints on the acceleration and propagation of cosmic rays in this region.

38th International Cosmic Ray Conference (ICRC2023)
26 July - 3 August, 2023
Nagoya, Japan



*Speaker

1. Introduction

Cosmic rays (CRs) are charged particles, mostly protons and atomic nuclei. With an energy density comparable to those of thermal gas and magnetic field in the Galaxy, they are an essential Galactic ingredient. Their interaction with dense interstellar matter has two important effects: 1) high-energy (>1 GeV) protons produce γ -rays by proton-proton interactions ; 2) low-energy (<1 GeV) cosmic rays ionize the gas and play a key role in the chemistry of the interstellar medium. To understand their influence in the Galaxy, it is necessary to know where CRs are accelerated and how they propagate. Indeed, the mechanisms behind their origin and acceleration remain elusive. Supernova remnants (SNRs) have long been suspected as the primary accelerators of Galactic cosmic-ray particles via diffusive shock acceleration processes [1]. SNRs are also known to emit non-thermal radiation in multiple forms: radio waves, X-rays, and γ -rays. If an SNR is located close to a molecular cloud, the γ -ray emission produced by the interaction between the freshly accelerated CR particles and the target reservoir of the molecular cloud will be enhanced. The recent observations of the SNRs IC 443, W44, W51C and W49B with the *Fermi*-LAT¹ telescope [2–4] support such a hadronic scenario, consistent with the so-called SNR paradigm for the origin of primary CRs in the Galaxy. Using γ -ray observations, a previous *Fermi*-LAT data analysis identified new regions where protons are being accelerated and interact with matter by detecting a characteristic signature in their γ -ray spectra. One of the best candidates is the HB3/W3 complex [5, 6] (distance of ~ 2 kpc), where HB3 is an SNR and W3 a molecular cloud and very active high-mass star forming region. HB3 (SNR G132.7+1.3) is considered to be an evolved SNR ($\sim 3 \times 10^4$ yr [7]) as it is one of the most extended ones [5, 8]. Its interaction with the W3 region has been studied with large scale CO observations (see [9] and references therein), and the SNR HB3 has been first detected in γ -rays in 2016 with 6 years of *Fermi*-LAT data [6].

2. *Fermi*-LAT data analysis and results

In this study, we analyzed 14 years of P8R3 data observed by the *Fermi*-LAT telescope in the HB3/W3 region. We define a $15^\circ \times 15^\circ$ region around the complex and include in our model all 4FGL sources located in a $25^\circ \times 25^\circ$ region centered on the HB3/W3 complex. Our analysis is based on the 4FGL-DR3 catalog [10], and has been carried out using the `FERMITOOLS 2.2.0` software and the `FERMIPY 1.2` python package. In the catalog, HB3 is referred to as 4FGL J0221.4+6241e and W3 as 4FGL J0222.4+6156e. In this analysis, we used `edisp_bins = -1` (between 1 GeV and 1 TeV) and `edisp_bins = -3` (between 100 MeV and 1 TeV) to account for the effect of energy dispersion. We used a pixel size of `binsz = 0.03°` and a maximum zenith angle of `zmax = 105°` (between 1 GeV and 1 TeV), and `binsz = 0.05°` and `zmax = 80°` (between 100 MeV and 1 TeV). We performed a binned likelihood analysis. The Galactic diffuse emission is modeled by the standard file `gll_iem_v07.fits` and the residual background and extragalactic radiation are described by an isotropic component, depending on the PSF event type, with the spectral shape in the tabulated model `iso_P8R3_SOURCE_V3_v1.txt`. The power-law spectral parameters of the Galactic diffuse and the normalization of isotropic components are fitted.

¹Large Area Telescope

2.1 Morphological analysis

The morphological analysis of the region was done between 1 GeV and 1 TeV using all PSF event types. Figure 1 shows the excess TS maps obtained. The left panel displays the excess TS map of both HB3 and W3, where the cyan contour represents the Dame ^{12}CO data from 2001 [11]. The Dame ^{12}CO template seems to correlate with the γ -ray emission, even if it appears that the maximum emission from this template is a little bit offset compared to the maximum of the γ -ray emission. Due to the difference in brightness between HB3 and W3, the SNR is here hidden by the molecular cloud. The right panel shows this time the excess TS map of HB3 only, where the magenta contour is the CGPS radio data, the green one is the ROSAT X-ray data and the cyan contour represents the Dame ^{12}CO template. HB3 discloses a bright γ -ray emission in the North. Different geometrical template shapes were tested for HB3 and our best template seems to be the uniform disk represented in white, slightly smaller than the one obtained by Katagiri et al. [6], represented in orange. Some point-like sources are added by FERMIPY where some hot spots with $\text{TS} > 16$ are found (see Table 1). The correlation between the CGPS radio data or the ROSAT X-ray data of HB3 and the γ -ray emission of the SNR is not clear, the radio template not being able to encompass all the Northern γ -ray emission and the X-ray one being bright further North and South.

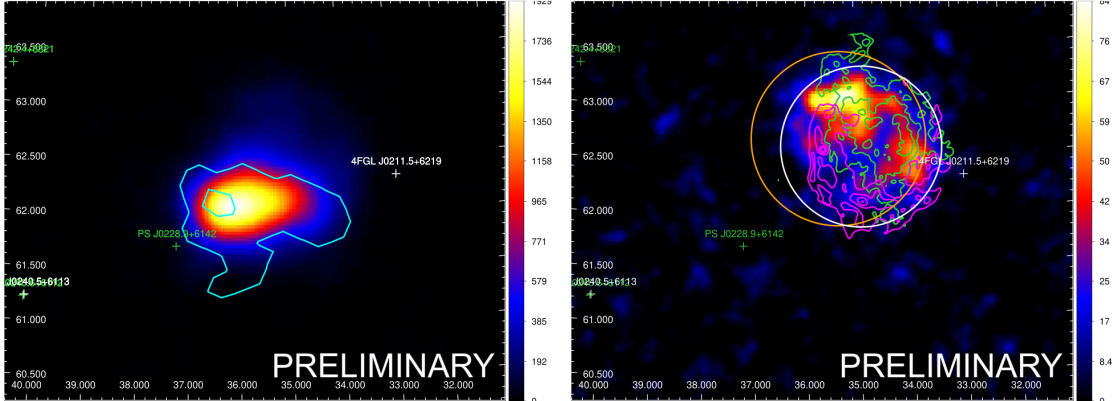


Figure 1: *Left panel:* Excess TS map (between 1 GeV and 1 TeV) of both HB3 and W3. The molecular cloud W3 is much brighter than the SNR, with almost a factor 10 between their TS values. The cyan contour is the Dame ^{12}CO template of W3 from 2001, which seems to correlate quite well with the γ -ray emission observed. *Right panel:* Excess TS map (between 1 GeV and 1 TeV) of the SNR HB3 only. The magenta contour is the CGPS radio data of HB3 and the green contour is the ROSAT X-ray template. The orange circle represents the disk reported in [6] for HB3, while the white circle is the best disk obtained in our analysis.

In order to improve our best model for W3, different divisions of the Dame template have been tested. We compared our different models using the Akaike Information Criterion (AIC) which enables to take into account the number of degrees of freedom and to compare even non-nested models. It is given by $AIC_i = 2k_i - 2\ln(L_i)$ where k is the number of degrees of freedom and L is the likelihood of the model tested (see Table 2, where we compute a ΔAIC). As there is an offset between the maximum of the γ -ray emission and the maximum of the ^{12}CO template, and as there was a point-like source added by FERMIPY in the middle of the molecular cloud, we first tried to

Source	RA (degrees)	DEC (degrees)
PS J0222.8+6202	35.71	62.04
PS J0228.9+6142	37.24	61.71
PS J0240.6+6112	40.16	61.22
PS J0242.4+6321	40.60	63.36

Table 1: Coordinates of the additional point-like sources added close to W3 and HB3 (within a 3° region around the HB3/W3 complex).

divide the Dame template into three equal parts, which improved significantly the likelihood. This allowed to remove the point source PS J0222.8+6202 as it is not significant anymore. Then, as the southern part of the Dame template shows no γ -ray emission, we tried to divide the Dame template into four parts, isolating this southern part, and the likelihood was again improved. Finally, we tried to split the brightest (East) part of the Dame template into two parts (as presented in Figure 2, right panel). This improved the likelihood significantly. Splitting the two other parts did not improve the likelihood further.

Templates	Log Likelihood value $\ln(L)$	number of d.o.f k	ΔAIC $= AIC_{4FGL} - AIC_i$
4FGL Disk (HB3) Dame (W3) (+ PS J0222.8+6202)	-1324843.4	10	0
ROSAT (HB3) Dame (W3) (+ PS J0222.8+6202)	-1324827.1	10	32.6
Radio + ROSAT (HB3) Dame (W3) (+ PS J0222.8+6202)	-1324802.3	11	80.2
Best Disk (HB3) Dame (W3) (+ PS J0222.8+6202)	-1324794.1	13	92.6
Best Disk (HB3) Dame divided in 3 (W3)	-1324781.0	15	114.8
Best Disk (HB3) Dame divided in 4 (W3)	-1324773.7	18	123.4
Best Disk (HB3) Dame divided in 5 (W3)	-1324762.5	21	139.8

Table 2: Comparison between the different template combinations used to reproduce the γ -ray morphology of HB3 and W3 (via the Akaike Information Criterion). The AIC value obtained with the best disk for HB3 from [6] used in the 4FGL catalog and the Dame template for W3 is here used as a reference to quantify the improvement of the different models tested. Please note that the first four tests require the addition of a point source (PS) within W3 modeled as a power-law (see Section 2.1). Except for the combination of ROSAT and Radio data, all components for W3 and HB3 are modeled with a log parabola.

2.2 Spectral analysis

The spectral analysis has been carried out between 100 MeV and 1 TeV relying on the best model obtained at the end of the morphological analysis. Here, the binned likelihood analysis includes only PSF2 and PSF3 events which are higher quality events. At this energy, the spectra of both HB3 and W3 are well fitted with a log parabola spectral model, which is described as:

$$\frac{dN}{dE} = N_0 \left(\frac{E}{E_b} \right)^{-(\alpha + \beta \ln(E/E_b))}$$

Figure 2 shows the Spectral Energy Distributions (SEDs) of the SNR HB3 as well as the ones of two of the five parts the molecular cloud W3 was divided into, called here W3_part and W3_full. W3_full is a part of W3 where there is a full overlap between the SNR and the molecular cloud, while in W3_part the overlap is only partial. Their spectral parameters are presented in Table 3, showing that W3_part and W3_full have different γ -ray spectral properties. To confirm this result, we performed a joint likelihood analysis of each pair of two sources among these three components using the composite likelihood tool, Composite2, of the Fermi Science Tools². Our likelihood analysis indicates that the spectra of W3_part and W3_full are significantly different at 4σ level. An evidence for spectral difference at 2.9σ level between HB3 and W3_full is also detected, while the spectra of HB3 and W3_part are very similar. While Katagiri et al. [6] concluded that the spectrum of W3 can be reproduced without any change from the proton momentum spectrum of the SNR HB3, we see that is it not the case if one analyzes smaller regions within the molecular cloud.

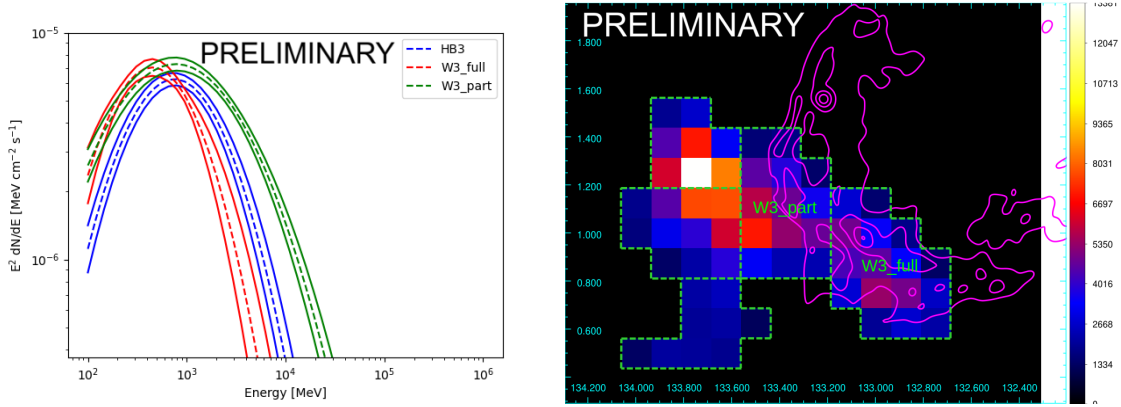


Figure 2: *Left panel:* Spectral Energy Distributions (SEDs) of HB3 (in blue), W3_full (in red) and W3_part (in green) obtained in the 100 MeV - 1 TeV energy band. The butterflies present the 1σ statistical error on the spectrum derived with our analysis for each region. *Right panel:* Dame ^{12}CO template used in this analysis and its associated division. The magenta contour is the CGPS radio data of HB3. The colour scale is an arbitrary rescale of the radio integrated intensity for velocities with respect to the local standard of rest between -44.2 km s^{-1} and -33.8 km s^{-1} as previously done by Katagiri et al. [6].

²Method allowing to compare two spectra. First, the three parameters (N_0 , α and β) are left free for both log parabola. Then both α and β values are tied together with a value consistent for both spectra, so that there are only four free parameters left instead of six at the beginning. The likelihood values of the two steps can then be compared to see if the difference between the spectra is significant or not.

Source	Prefactor ($\text{MeV}^{-1} \text{cm}^{-2} \text{s}^{-1}$)	α	β	E_b (GeV)
HB3	$(1.41 \pm 0.13) \times 10^{-12}$	2.77 ± 0.17	0.43 ± 0.09	1.8
W3_full	$(5.09 \pm 0.38) \times 10^{-12}$	2.79 ± 0.14	0.48 ± 0.10	1.0
W3_part	$(7.17 \pm 0.55) \times 10^{-12}$	2.12 ± 0.09	0.25 ± 0.05	1.0

Table 3: Best fit values for the log parabola of HB3, W3_full and W3_part in the 100 MeV - 1 TeV energy band. Only statistical errors are provided.

3. Conclusions

In this study, we analyzed 14 years of *Fermi*-LAT data in order to study the γ -ray emission of the HB3/W3 complex. The morphological analysis (performed between 1 GeV and 1 TeV) of HB3 and W3 shows a bright γ -ray emission in the northern part of the SNR. The best model obtained for W3 seems to be the Dame ^{12}CO template, divided into five parts. For HB3, despite multiple template tests, the best template seems to be a uniform disk, different than the one previously found by Katagiri et al. [6] in 2016 with 6 years of *Fermi*-LAT data. The spectral analysis (performed between 100 MeV and 1 TeV) shows significant differences between the spectra of HB3 and sub-regions within the cloud W3 itself.

We still need to understand where the differences observed between the SEDs come from. Peron et al [12] proposed for the SNR W44 that they could originate from: an intrinsic asymmetry in the shock, propagation effects, or irregularities in the interstellar medium.

Acknowledgments

The *Fermi*-LAT Collaboration acknowledges support for LAT development, operation and data analysis from NASA and DOE (United States), CEA/Irfu and IN2P3/CNRS (France), ASI and INFN (Italy), MEXT, KEK, and JAXA (Japan), and the K.A. Wallenberg Foundation, the Swedish Research Council and the National Space Board (Sweden). Science analysis support in the operations phase from INAF (Italy) and CNES (France) is also gratefully acknowledged. This work performed in part under DOE Contract DE-AC02-76SF00515.

MLG acknowledges support from Agence Nationale de la Recherche (grant ANR- 17-CE31-0014). MLG and AC also acknowledge support from the RRI Origins.

References

- [1] Drury, L 1983, Space Science Reviews, Volume 36, Issue 1, pp.57-60
- [2] Ackermann, M., Ajello, M., Allafort, A., et al. 2013, Science, 339, 807
- [3] Jogler, T., & Funk, S. 2016, ApJ, 816, 100
- [4] H. E. S. S. Collaboration, Abdalla, H., Abramowski, A., et al. 2018, A&A, 612, A5
- [5] Routledge, D., Dewdney, P. E., Landecker, T. L., et al. 1991, A&A, 247, 529
- [6] Katagiri, H., Yoshida, K., Ballet, J., et al. 2016, ApJ, 818, 114
- [7] Lazendic, J. S., & Slane, P. O. 2006, ApJ, 647, 350

- [8] Fesen, R. A., Downes, R. A., Wallace, D., et al. 1995, *AJ*, 110, 2876
- [9] Bieging, J. H., & Peters, W. L. 2011, *ApJS*, 196, 18
- [10] Ajello, M., et al. 2022, *ApJ Supplement Series*, 263:24
- [11] Dame, T. M., Hartmann, D., & Thaddeus, P. 2001, *ApJ*, 547:792-813
- [12] Peron, G., Aharonian¹, F., Casanova, S., Zanin, R., & Romoli, C. 2020, *ApJL*, 896 L23